

Expression and Regulation of the Retinoic Acid Synthetic Enzyme RALDH-2 in the Embryonic Chicken Wing

KIRSTEN BERGGREN,¹ ELIZABETH B. EZERMAN,¹ PETER MCCAFFERY,² AND CYNTHIA J. FOREHAND^{1*}

¹University of Vermont, Department of Anatomy and Neurobiology, Burlington, Vermont

²E.K. Shriver Center, Waltham, Massachusetts

ABSTRACT Retinaldehyde dehydrogenase type 2 (RALDH-2) is a major retinoic acid (RA) generating enzyme in the embryo. Here, we report immunolocalization of this enzyme (RALDH-2-IR) in the developing wings of stage 17–30 chicken embryos. RALDH-2-IR is located in the area of the presumptive muscle masses, although it is not colocalized with developing muscle cells. RALDH-2-IR is located in tendon precursor cells and may be present in muscular connective tissue. We show that motor neurons and blood vessels, tissues showing RALDH-2-IR as they enter the limb, are capable of synthesizing and releasing RA in culture. RALDH-2-IR in the limb mesenchyme is under the control of both the vasculature and the motor innervation; it is decreased with denervation and increased with hypervascularization. RALDH-2-IR is present in the motor neuron pool of the brachial spinal cord, but this expression pattern is apparently not under the control of limb target tissues, RA in the periphery, or somitic factors. RA is known to be a potent inducer of cellular differentiation; we propose that locally synthesized RA may be involved in aspects of wing tissue specification, including cartilage condensation and outgrowth, skeletal muscle differentiation, and recruitment of smooth muscle cells to the vasculature. © 2001 Wiley-Liss, Inc.

Key words: limb development; mesenchymal specification; retinaldehyde dehydrogenase; retinoic acid; vascular development

INTRODUCTION

Retinoic acid (RA) is involved in many aspects of tissue specification and differentiation during embryonic development. RA is involved in the early axial patterning of the limb and determination of the anterior-posterior (A-P) patterning (Tickle et al., 1982, 1985; Eichele, 1989; Helms et al., 1996; Lu et al., 1997; Stratford et al., 1999). RA is also involved in limb bud outgrowth (Stratford et al., 1996; Power et al., 1999). Efforts to pinpoint the sites of activity of RA in the developing limb have focused on localization of RA receptors (Dollé et al., 1989, 1994; Ruberte et al., 1990; Mendelsohn et al., 1991), knockouts of RA receptors (Lohnes et al., 1993; Mendelsohn et al., 1994) and high

performance liquid chromatography studies (Thaller and Eichele, 1987, 1990; Maden et al., 1998). However, the ubiquitous nature of many of these receptors and low physiological levels of RA have made it difficult to localize RA activity within the embryo with these methods. We and others have previously reported the general localization pattern of the RA synthetic enzyme, retinaldehyde dehydrogenase-2 (RALDH-2), which is the primary synthetic agent for RA in the developing embryo (Zhao et al., 1996; Niederreither et al., 1997, 1999; Berggren et al., 1999). Tissues that express RALDH-2 synthesize RA (McCaffery and Dräger, 1994; Berggren et al., 1999), and RALDH-2 knockout mice are deficient in RA (Niederreither et al., 1999); thus, RALDH-2 seems to be a vital enzyme responsible for RA synthesis in the embryo. Therefore, localization of RALDH-2 immunoreactivity (RALDH-2-IR) can be used as a tool to pinpoint regions of synthesis of endogenous RA. In this study, we have used the distribution of RALDH-2-IR in the developing chicken wing to examine possible sources of RA in the differentiating mesenchyme during Hamburger and Hamilton (H&H) stages 17–30 (Hamburger and Hamilton, 1951).

That RA is required for normal limb development is well established. Subsequent to the initial axial patterning and induction events, RA may be required for the maintenance of limb outgrowth and development of skeletal elements. Double-mutant mouse embryos missing both the α and γ RA receptor subtypes show that, although the initial axial patterning of the limb is not altered, limb deformities in several of the later-forming structures occur, most markedly in the forelimb (Lohnes et al., 1994). Forelimb buds are shortened, the radius and ulna are curved, and carpals and phalanges are malformed. These findings indicate a role for RA in later forelimb development, although to date, sources of RA in the limb at these stages have not been identified. Here, we seek to identify the sources of RA by mapping the distribution of RALDH-2-IR in the chicken embryo wing at the cellular level.

Grant sponsor: NIH; Grant number: NS30062; Grant number: HD05515; Grant number: HD01179.

*Correspondence to: Cynthia J. Forehand, University of Vermont, Department of Anatomy and Neurobiology, Burlington, VT 05405. E-mail: cforehan@zoo.uvm.edu

Received 21 November 2000; Accepted 3 May 2001

We also investigate whether the RALDH-2-IR observed in the limb mesenchyme is under neuronal influence. As previously reported, RALDH-2 is observed in the motor neurons at the levels of the limbs (Zhao et al., 1996; Niederreither et al., 1997; Sockanathan and Jessell, 1998) and in the motor axons extending into the limb (Berggren et al., 1999), suggesting a possible source of RA in the limb. Although most studies of the role of the nerve in limb morphogenesis have focused on the differentiation of muscle fiber types and the proliferation of skeletal muscle (Phillips and Bennett, 1984; Fredette and Landmesser, 1991), studies on developing tadpoles have found that denervation also decreases the rate of bone maturation (Dietz, 1987). Thus, it seems likely that innervation of the limbs is necessary for both muscle and bone development. RA is a factor that could mediate this neuronal influence; we examine whether levels of RALDH-2 in the wing are altered after denervation and whether motor neurons in culture release RA.

RA may also play a role in differentiation of the developing vasculature. When treated with appropriate levels of RA, undifferentiated embryonal carcinoma cells (P19) take on many of the structural and genetic characteristics of smooth muscle cells (Blank et al., 1995) and themselves express the RA synthetic enzyme RALDH-2 (Zhao et al., 1996). It has been suggested that RA is involved in the recruitment of smooth muscle cells from the surrounding undifferentiated mesenchyme (as discussed in Hirschi et al., 1998). We have investigated the localization of RALDH-2-IR in the walls of blood vessels entering the wing at the same time as the motor axons. The RA synthetic ability of these blood vessels could provide another source of RA in the limbs.

The primary role for RA in limb development has been considered to be the regulation of initial outgrowth and axial patterning. We present evidence for an additional later role in tissue specification. We demonstrate that RA is synthesized in the wing in a spatiotemporally regulated manner, in areas of the limb known to be sensitive to retinoid exposure. Additionally, we show that tissues entering the wing at this time are capable of releasing RA. We propose that RA synthesis by RALDH-2 in the developing limb plays a vital role in the maturation of many limb structures and that the localization and regulation of RALDH-2-IR in the wing can be used to further explore the role of RA in the later maturation of the limbs.

RESULTS

Distribution of RALDH-2 Immunoreactivity in the Wing Bud

Here, we describe the normal distribution of RALDH-2-IR in the developing chicken embryo wing between stages 17, when limb bud outgrowth begins, and stage 30, when the limb bud is well specified and most of the adult structures are recognizable. At stage 17, the lateral mesoderm shows strong RALDH-2-IR,

which is continuous with the RALDH-2-IR seen in the early wing bud (Fig. 1A). The RALDH-2-IR in the wing fades gradually between stage 17 and stage 19, with lowest levels in the center of the limb and slightly higher levels in the most anterior and posterior regions of the limb, which are adjacent to the strongly RALDH-2-IR nonlimb lateral mesoderm. There was no apparent overall gradient of RALDH-2-IR in the A-P, dorsal-ventral or proximal-distal axes. By late stage 19/early stage 20, the RALDH-2-IR in the wing is greatly reduced (Fig. 1B) and is negligible by the end of stage 20. As the motor neurons grow out toward the wing bud, there is an area of RALDH-2-IR that can be seen at the site of the presumptive brachial plexus (BP in Fig. 1B). This area labels strongly by the time the axon tips reach the brachial plexus at stage 23 (Fig. 1C). The motor neurons then extend into the undifferentiated wing mesenchymal tissue, splitting into dorsal and ventral branches to their respective muscle groups. At stage 25, RALDH-2-IR extends into the wing adjacent to the axon tips (Fig. 1D). There is also RALDH-2-IR in a region at the tip of the wing bud, just proximal to the apical ectodermal ridge (AER), but distal to, and not in contact with, the tips of the axons. RALDH-2-IR is also present surrounding some of the blood vessels (Fig. 1E, see also discussion of vasculature below). By stage 27–30, RALDH-2-IR is more diffuse through the entire wing (Fig. 1E). There are locally higher levels of RALDH-2-IR in some areas, but the pattern of this localization is not obviously associated with identifiable structures. As the cartilage begins to condense, RALDH-2-IR is distinctly absent from the cartilage, although it is strong in the perichondrial tissues. RALDH-2-IR is negligible in the ectoderm at every stage examined.

As discussed previously (Berggren et al., 1999), RALDH-2-IR is also seen in the motor neurons of the brachial and lumbar regions. We see RALDH-2-IR not only in the motor neuron cell bodies, as has been reported elsewhere (Niederreither et al., 1999; Sockanathan and Jessell, 1998), but also in the axons as they extend into the limbs (Fig. 1B–D). Sensory neurons in the dorsal root ganglia (DRG) do not label for RALDH-2, nor do their axons (Fig. 1D).

Tissue Specificity of RALDH-2-IR

Muscle and connective tissue. The localization of mesenchymal RALDH-2-IR around the tips of the motor axons, which are known to be extending into developing skeletal muscle, indicated that the developing muscle itself could be labeling for RALDH-2. Stains with ALD-66, a monoclonal antibody for slow muscle myosin, revealed that in the stages we examined, immunoreactivity for ALD-66 (ALD-66-IR) was present in areas surrounding the axon tips, similar to the distribution of RALDH-2-IR (Fig. 2A). Expression of RALDH-2-IR and ALD-66-IR overlapped when examined under the fluorescence microscope, but examination with confocal microscopy showed that the elon-

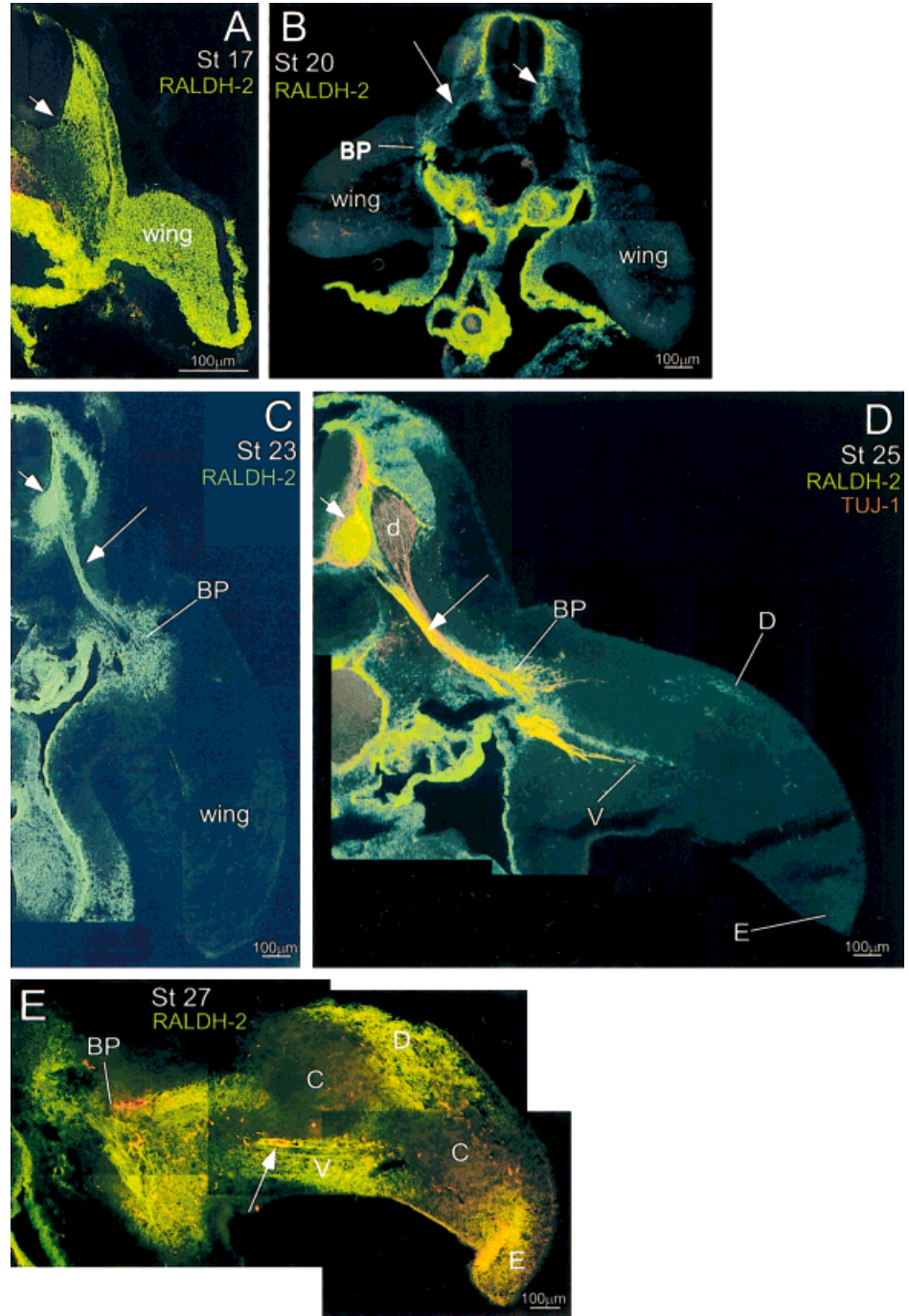


Fig. 1. Normal series showing retinaldehyde dehydrogenase type 2 immunoreactivity (RALDH-2-IR) (green) in the developing wing. **A:** Stage (St) 17 chicken embryo section. The short arrow indicates motor neuron (mn) cell bodies in the neural tube. **B:** Stage 20 wing section, RALDH-2-IR is greatly diminished in the wing but can be seen at the site of the brachial plexus. The long arrow indicates RALDH-2-IR in motor axons. Short arrow, mn; BP, brachial plexus. **C:** Stage 23 wing section, RALDH-2-IR is present in the brachial plexus but not in the rest of the wing. Long arrow, axons; short arrow, mn. **D:** Stage 25 wing section, RALDH-2-IR is present surrounding the axon tips as they extend into the wing. D, RALDH-2-IR surrounding the dorsal nerve branch; V, RALDH-2-IR surrounding the ventral nerve branch; E, RALDH-2-IR at the distal end of the wing bud. Yellow color in motor axons (long arrow) results from colocalization of RALDH-2-IR and TUJ-1 (red). Sensory neurons in the dorsal root ganglion (d) label only with TUJ-1. Short arrow, mn; BP, brachial plexus. **E:** Stage 27 wing section. RALDH-2-IR is more extensive in the wing bud, in the mesenchyme of the dorsal (D) and ventral (V) pre-muscle masses, in the brachial plexus (BP), and at the distal end of the wing (E). Yellow color near E is due to a fold in the tissue. RALDH-2-IR is absent from condensing cartilage (C). Arrow, blood vessel.

gated immunoreactive myosin fibers were always distinct from the rounded cytoplasmic accumulations of RALDH-2 (Fig. 2B).

Another muscle protein, desmin, is present in post-mitotic myoblasts as well as in myotubes. Desmin localizes to Z-discs in mature myotubes, but is present throughout the entire cell in the undifferentiated myoblasts, and may stain muscle precursors earlier than the specific slow-muscle myosin stained by ALD-66. By using a monoclonal antibody for desmin, we found a

similar distribution to that seen for myosin. RALDH-2-IR and desmin-IR were often in the same region of tissue but did not colocalize within the same cells (Fig. 2E). Additionally, the desmin-IR develops later in development than RALDH-2-IR; only faint wisps of desmin-IR are seen at stage 25 (not shown), a stage at which RALDH-2-IR is already extensive in the wing.

To examine earlier time points and undifferentiated muscle precursor cells, we used a monoclonal antibody to the Pax-7 gene, which is expressed in

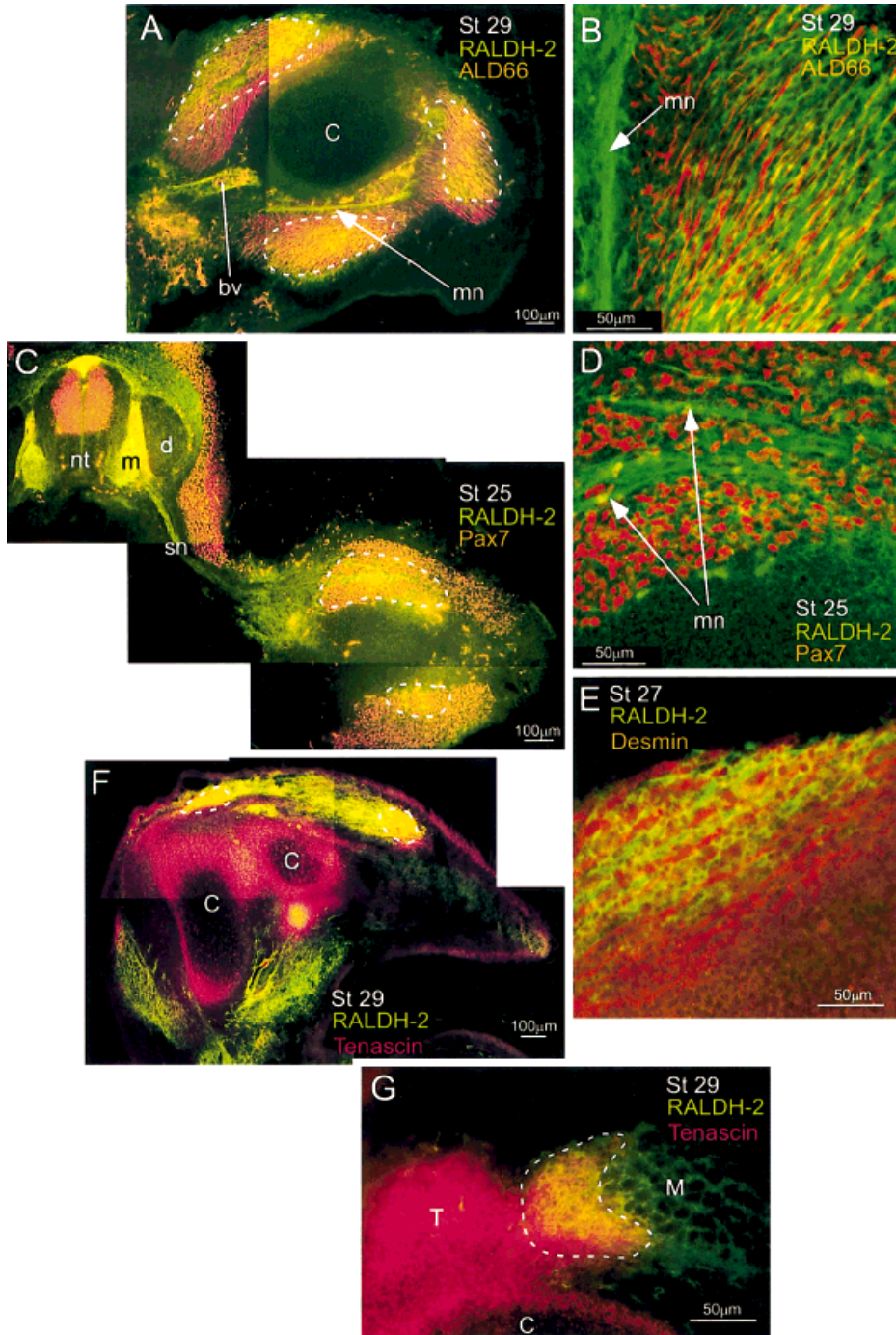


Fig. 2. Colocalization of retinaldehyde dehydrogenase type 2 immunoreactivity (RALDH-2-IR) (green) and other cellular markers. **A:** Stage (St) 29 wing section showing immunoreactivity for RALDH-2 and the muscle myosin marker ALD66 (red). Both stains are excluded from the condensing cartilage (C), and colocalize in the developing muscle masses (areas of colocalization are traced by dashed lines). bv, blood vessel; mn, motor axons. **B:** Confocal microscope image of the same section as A, showing that ALD66 and RALDH-2 do not localize to the same cells. **C:** Stage 25 wing section stained for RALDH-2-IR and Pax7-IR (red). Areas of overlapping stain are traced by dashed lines. nt, neural tube; m, motor neuron cell bodies; d, dorsal root ganglion; sn, spinal nerve. **D:** Confocal image of the same section as C showing motor axons (mn) coursing through Pax7 cells as well as RALDH-2-IR distinct from Pax7-IR cells. **E:** Confocal image of stage 27 wing section showing stain for RALDH-2 and desmin (red). Although there is regional overlap, there is not cellular colocalization of RALDH-2-IR and desmin-IR. **F:** Stage 29 wing section showing IR for RALDH-2 and the tendon marker tenascin (red). Both are excluded from the condensing cartilage (C). Tenascin is not seen in the muscle masses, but there is an area of overlap (dashed lines) at the interface of the tendon and muscle. **G:** Confocal image of the same section as F. Note area of double-labeled fibers (dashed circle) between the tendon (T) and muscle (M) precursors.

migrating premyogenic cells (Goulding and Gruss, 1989). These cells had a broader distribution than RALDH-2-IR and preceded RALDH-2-IR into the wing, with Pax-7-IR cells observed in the wing at stage 23. Pax-7-IR cells also extended into the wing distal to the extent of RALDH-2-IR (Fig. 2C), and, although there was some overlap in regions of immunoreactivity, confocal microscopy again reveals no double-labeled cells (Fig. 2D).

Because RALDH-2-IR is in the same area as skeletal muscle, in tissues intermixed with the muscle cells, connective tissue is likely to show RALDH-2-IR. A recent description of tenascin localization by Kardon (1998) showed a pattern of this early tendon marker that appeared similar to that observed for RALDH-2-IR. Tenascin is located adjacent to the condensing cartilage elements and extends into the area of presumptive muscle masses. Colocalization of RALDH-2-IR and tenascin-IR

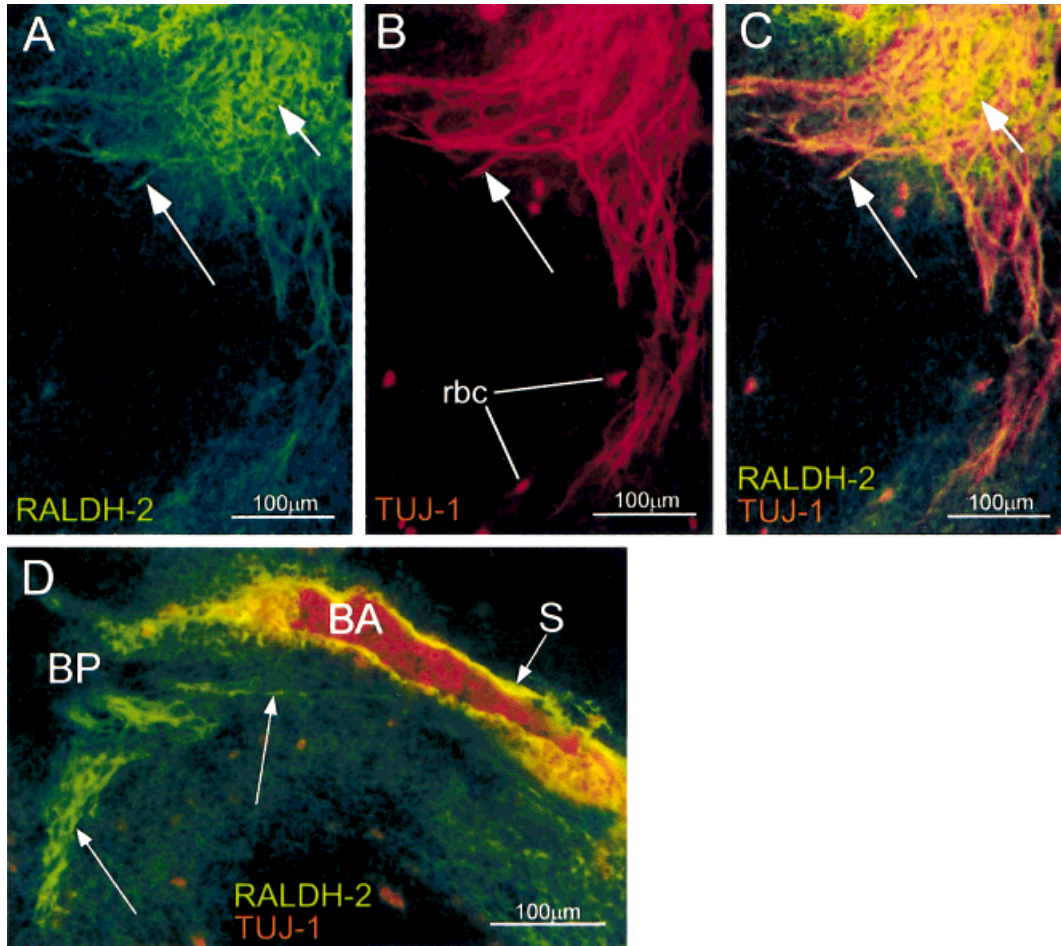


Fig. 3. Axons and blood vessels in the brachial plexus of stage 24 chicken embryo wing sections. **A:** Retinaldehyde dehydrogenase type 2 immunoreactivity (RALDH-2-IR) (green) seen in the motor axons (long arrow) and mesenchyme (short arrow) of the brachial plexus. **B:** TUJ-1 labeling all axons in the brachial plexus (long arrow indicates one axon).

rbc, autofluorescent red blood cells in capillaries of the plexus. **C:** Colocalization of RALDH-2 and TUJ-1. Most axons label for both stains (long arrow). Short arrow, RALDH-2-IR mesenchyme. **D:** Brachial artery (BA) passing through the plexus (BP). RALDH-2-IR is present in motor axons (long arrows) and in the vascular smooth muscle (S).

showed that there was indeed some overlap at the interface between the tenascin and RALDH-2 areas (Fig. 2F). Confocal microscopy reveals that the area of overlap is not extensive, but there are fibrous extensions from the RALDH-2-IR cells that also label for tenascin at the interface between the two (Fig. 2G). Therefore, the areas of RALDH-2-IR adjacent to cartilage appear to be tendon precursor tissue, but the identity of the RALDH-2-IR cells within the muscle masses is still unknown.

Motor axons and blood vessel walls. Motor axons extending into the wing exhibit RALDH-2-IR along their entire length, from the time they emerge from the neural tube through stage 30 (later stages were not examined). An examination of stage 24 brachial plexus shows the location of RALDH-2-IR in the motor axons (Fig. 3A) precisely colocalized with the neural specific tubulin marker TUJ-1 (Fig. 3B,C). More neuronal processes are labeled for TUJ-1 than for RALDH-2, because the sensory axons extending from DRG neurons do not exhibit RALDH-2-IR.

RALDH-2-IR is also present in the walls of the blood vessels entering the wing. Blood vessels in other parts of the embryo also show RALDH-2-IR, but aside from the aorta, these were not closely examined. The capillaries at the distal part of the wing did not have detectable RALDH-2-IR, but the larger vessels branching from the brachial artery showed RALDH-2-IR in a single cell layer surrounding the blood vessels (Fig. 3D).

Vascular smooth muscle. Beginning at stage 25, when blood vessels are invading the developing wing, RALDH-2-IR is observed in the walls of many of these vessels, as well as in tissue immediately surrounding the vessels. Double labeling with antibodies to RALDH-2 and α -smooth muscle actin (α -actin) shows that there is a single cell layer of α -actin-IR cells (vascular smooth muscle cells) closer to the lumen than the area of RALDH-2-IR (Fig. 4A–C). This observation indicates that RALDH-2 is not located in endothelial cells of the vasculature, as endothelial cells are the inner-

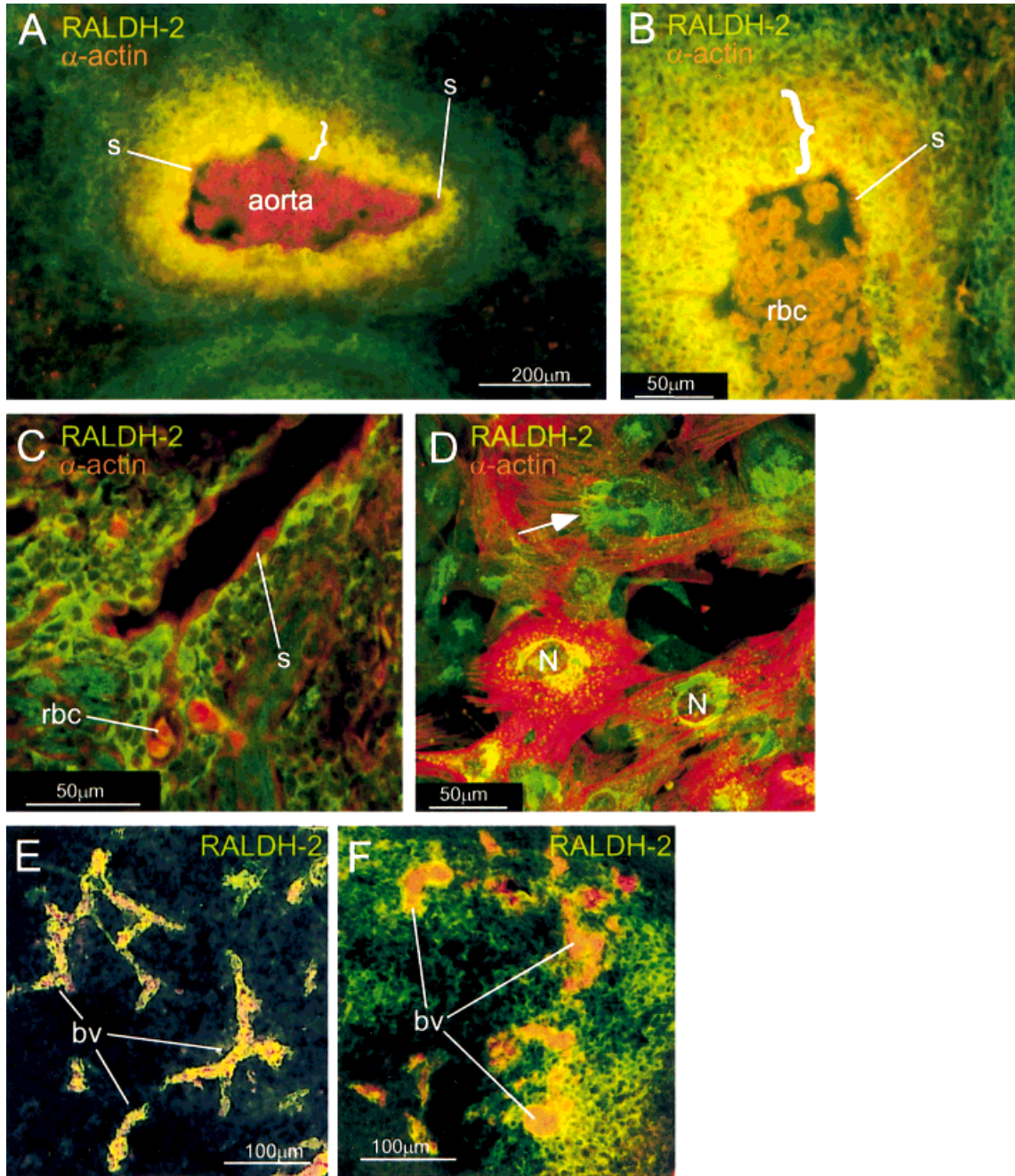


Fig. 4. Retinaldehyde dehydrogenase type 2 immunoreactivity (RALDH-2-IR) in vascular smooth muscle and mesenchyme surrounding blood vessels. **A:** Stage 27 aorta showing smooth muscle cell lining (s) surrounded by a layer of cells double labeled for α -smooth muscle actin and RALDH-2 (indicated by white bracket). Further distally from the lumen of the aorta, RALDH-2-IR alone is observed in the mesenchyme. The lumen of the aorta is filled with red blood cells, which autofluoresce red. **B:** Confocal photomicrograph of a section adjacent to the section in A. s, α -smooth muscle actin labeled single layer of smooth muscle cells; bracket, area of smooth muscle cells also showing RALDH-2-IR; rbc, red blood cells. **C:** Artery in the brachial region of a stage 25 embryo. s, layer of smooth muscle cells within the area of RALDH-2-IR; rbc, red blood cell.

D: Smooth muscle cells grown in culture and stained for RALDH-2 (green) and α -smooth muscle actin (red). RALDH-2 localizes around the nucleus (N) of the cultured cells, whereas α -actin has a broader distribution throughout the cytoplasm. Note that some α -actin staining appears to be in nuclear regions (left marked nucleus) due to flattening of cytoplasm over the nucleus of intact cells. **E:** Blood vessels (bv) in a stage 25 wing grown on the CAM without innervation. Each blood vessel has RALDH-2-IR around the lumen, but RALDH-2-IR is not extensive in the mesenchyme. **F:** Blood vessels in a stage 28 wing grown on the CAM. Blood vessels show RALDH-2-IR in their walls, and there is extensive RALDH-2-IR in the wing mesenchyme.

most layer in the blood vessels, and are not visible in these preparations. Surrounding the layer of α -actin-IR cells is a multicellular layer of double-labeled cells (Fig. 4A,B), immunoreactive for both α -actin and RALDH-2. Surrounding the layer of double-labeled cells are mesenchymal cells labeling for RALDH-2 only, which are still in close association with the vessel.

To confirm that immature vascular smooth muscle cells are indeed making the RALDH-2 protein, smooth muscle cells grown in culture were stained for RALDH-2 and α -actin. The flattened morphology of these cells allows for a better localization of RALDH-2-IR within the cells. The cultured cells exhibit RALDH-2-IR in a region adjacent to and surrounding the nucleus but excluded from the nucleus itself and not extending into the distal regions of the cell (Fig. 4D). In contrast, α -actin immunoreactivity is present throughout the cell cytoplasm. No staining was observed in control cultures processed without primary antibody (not shown).

Putative RA Release From Motor Neurons and Blood Vessels

Motor neurons of the brachial region exhibit RALDH-2-IR in their cell bodies (Fig. 2 and Sockanathan and Jessell, 1998; Berggren et al., 1999), and also in their axon projections into the wing (Berggren et al., 1999, and figure 3A–C). We designed experiments to determine whether RA is released from motor neurons; to determine whether motoneuron RALDH-2 can provide a source of RA in the wing. Similarly, RALDH-2 expression in vascular walls suggests a vascular source of RA in the limb. RALDH-2-IR is apparent in the vessels of the chorioallantoic membrane (CAM) as well as those in the limb and aorta. As CAM vessels are easier to isolate, we used these vessels to explore vascular synthesis of RA.

To determine whether motor axons and blood vessels exhibiting RALDH-2-IR as they migrate into the wing are capable of releasing RA, we dissected and isolated these tissues, maintained them in culture overnight, and assayed for RA in the culture supernatant with the RA responsive cell line previously described (Sil 15 cells, Wagner et al., 1992; McCaffery and Dräger, 1997). We used hindbrain neurons as a control, as RALDH-2-IR is not detectable in the hindbrain after stage 20 (Berggren et al., 1999). Spinal meninges were also assayed, as they are a tissue with strong RALDH-2-IR throughout development (Berggren et al., 1999). Table 1 shows that RA was released by all of the RALDH-2-IR tissues examined: isolated motor neurons, isolated blood vessels, and the meninges from the brachial region of the spinal cord. All of these tissues release RA without the addition of substrate (retinal, retinol, or NAD), demonstrating that not only is the RA synthetic enzyme present and active in these tissues but also that the retinaldehyde precursor of RA is present. It should also be noted that the dissected meninges are capable of synthesizing RA in significant

TABLE 1. RA Synthesis/Release From Isolated Motor Neurons, Blood Vessels, and Meninges of E7 Chicken Embryos^a

Tissue	pM RA/ μ g protein ^b
Spinal motoneurons	44 \pm 5.6
Hindbrain motoneurons	Not detectable
Blood vessels-sample 1	24 \pm 0.6
Blood vessels-sample 2	6 \pm 0.9
Spinal meninges	13 \pm 1.4

^aA colorimetric assay of retinoic acid (RA) content was performed with Sil-15 RA-responsive cells, with intensity of β -gal expression quantified to show relative amounts of RA. Values are expressed as mean \pm SEM with assays done in triplicate. E7, embryonic day 7.

^bDetermined from a standard curve.

quantities, suggesting a source of RA contamination when assaying spinal cord sections for RA.

To better illustrate the release of RA from isolated motor neurons, the motor neurons were cultured with varying densities of RA responsive cells (Fig. 5A,B). Although it is not possible to determine conclusively whether the RA released is from the cell bodies of the neurons or from the axons, the coculture of neurons with a low density of responsive cells shows several examples of responsive cells in contact with only the processes of the motor neurons (Fig. 5B), strongly suggesting that RA is being released from the neuronal processes as well as from the cell bodies. Cultures of hindbrain neurons with responsive cells showed only minimal response (Fig. 5C). Cocultures with high densities of response cells show the overall *lacZ* response of Sil 15 cells to motor neurons is far greater than to control hindbrain neurons (Fig. 5D), again indicating a high level of RA release from motor neurons.

Sections of CAM blood vessels were also cocultured overnight with RA responsive cells in culture dishes. Figure 5E shows an area of RA responsive cells that had been directly beneath a section of blood vessel, showing that RA was released from the blood vessel during the incubation, confirming that the RALDH-2-IR cells in the vessel wall are capable of releasing RA.

Control of RALDH-2 in the Wing

Although there is a small amount of RALDH-2-IR in the mesenchyme surrounding blood vessels in the wing, the more striking pattern is that of RALDH-2-IR surrounding the axon tips. This staining is coincident with the arrival of the motor axons in the wing. To examine whether RALDH-2 in the wing is under the control of the motor axons, we investigated RALDH-2-IR in the absence of motor neuron innervation. To remove all motor innervation of the wing and brachial region, the neural tubes from embryos of stage 15–16 were removed adjacent to somites 13–21. Because the neural crest has already migrated at this stage, DRGs form normally, and sensory axons are present in the wing as evidenced by TUJ-1 staining. Embryos were

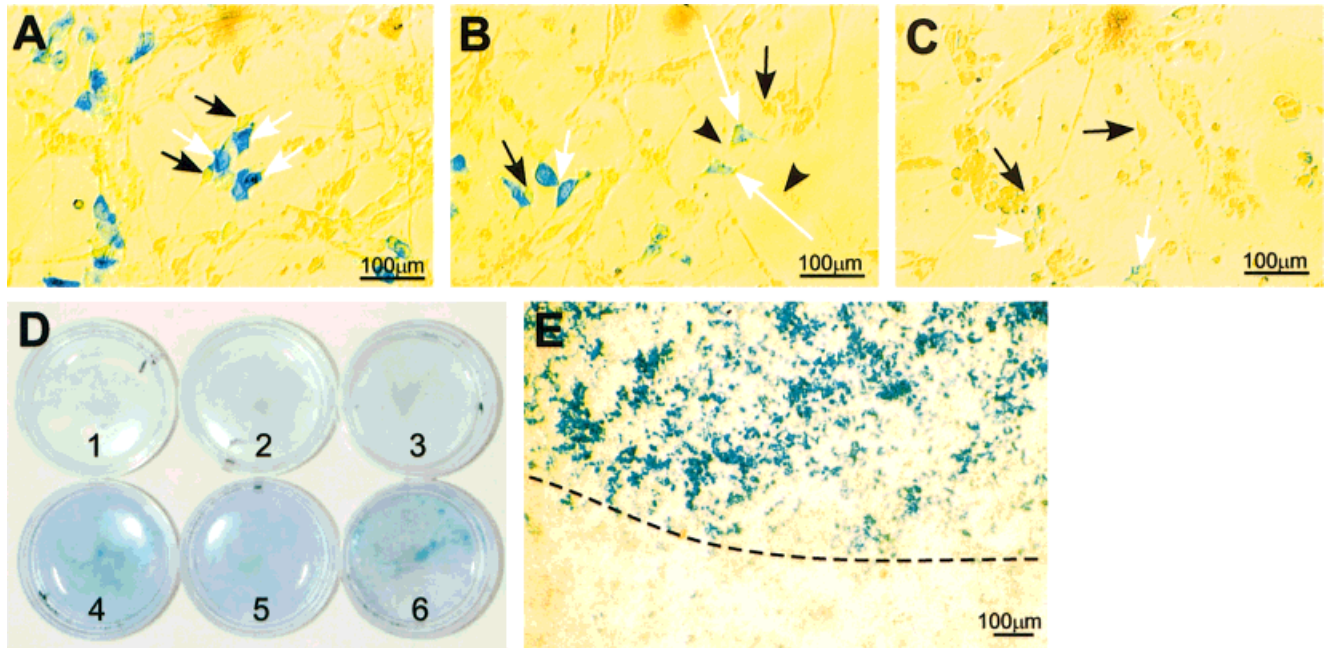


Fig. 5. Response of Sil-15 retinoic acid (RA) responsive cells to motor neurons and blood vessels. A-C contain low densities of responsive cells. **A:** Motor neurons and responsive cells cocultured overnight. Black arrows indicate motor neuron cell bodies; white arrows show adjacent responsive cells developed for β -gal reaction product, indicating release of RA from the motor neurons. **B:** Responsive cells adjacent to neuronal processes; long white arrows indicate responding cells adjacent to processes; black arrowheads indicate neuronal processes; black arrows, neuron cell bodies; short white arrow, responsive Sil-15 cells. **C:** Control

coculture of hindbrain neurons with RA responsive cells. Black arrows indicate neurons; white arrows indicate cells with background response levels. D and E contain high densities of responsive cells. **D:** Culture dishes containing hindbrain neurons and RA responsive cells (1-3) and motor neurons and RA responsive cells (4-6), showing response to RA released by motor neurons compared with background response to the non-RA-releasing hindbrain cells. **E:** RA-responsive cells after coculture overnight with a section of blood vessel. The blood vessel segment overlaid the cells in the area above the dashed line.

assayed at stage 25/26 for total wing RALDH-2-IR volume by using a Lucivid camera system and NeuroLucida Software (MicroBrightField, Inc.) to trace and measure the two-dimensional area of mesenchymal RALDH-2-IR in each section. RALDH-2-IR was significantly decreased at stage 26 in the denervated embryos, although not entirely absent (Fig. 6; Table 2). The denervated embryos still showed RALDH-2-IR surrounding blood vessels. As the blood vessels often run along with the nerves, the location of the RALDH-2-IR was similar between controls and denervated animals. However, the size of the area of immunolocalization was greatly reduced in the denervated animals compared with controls (Fig. 6A,B). The region of RALDH-2-IR at the distal end of the wing was also maintained in the denervated animals. By Stage 28, the RALDH-2-IR was similar between denervated and control animals (not shown); thus, the effect of denervation on RALDH-2-IR is transient, coincident with the time when the motor neurons are first invading the limb mesenchyme.

We also examined the expression pattern of tenascin in the denervated wings, as tenascin was the cellular marker found to be colocalized with RALDH-2. At stage 26, when the motor axons are newly arrived in the wing, there is a very small amount of tenascin present

at the most proximal wing bud, which is not altered with denervation. At stage 28, mesenchymal RALDH-2-IR is similar between denervated and control animals, and the relationship between RALDH-2-IR and tenascin-IR appears unchanged by denervation (not shown).

Because RALDH-2-IR was present near blood vessels in the denervated animals, the effects of vascularization on the development of RALDH-2-IR in the wing were examined. To assess the effects of exogenous hyper-vascularization on RALDH-2-IR, wing buds were grafted to the CAM of more mature embryos and allowed to grow. These wings develop normal morphology without innervation, but the vessels of the CAM eventually invade the grafted wing in excess of normal patterns of vascularization. Stage 25 CAM-grafted wings showed an invasion of many small vessels into the wing, and most of these vessels showed RALDH-2-IR in their walls (Fig. 4E). The amount of RALDH-2-IR in the wing mesenchyme was not noticeably increased at this time compared with denervated wings. However, by stage 28/29, the wings showed patterns of marked hypervascularization, along with increased areas of RALDH-2-IR in the mesenchyme surrounding these vessels (Fig. 4F). These data suggest that RALDH-2-IR in the wing is not solely dependent on

Fig. 6. Decrease in wing mesenchymal retinaldehyde dehydrogenase type 2 immunoreactivity (RALDH-2-IR) seen after motor denervation. **A:** Stage (St) 26 control wing section. Dorsal (D), ventral (V), and distal (E) mesenchymal RALDH-2-IR is seen in relation to the dorsal (db) and ventral (vb) nerve branches. NT, neural tube; m, motor neurons; d, dorsal root ganglia; sn, spinal nerve; A, aorta; M, mesonephros. **B:** Decrease in the area of RALDH-2-IR after motor denervation in a stage 26 embryo that had been denervated at stage 16. Sensory nerves stained with TUJ-1 are present in axial regions (TUJ-1 stain, short arrow) but very sparse in the wing.

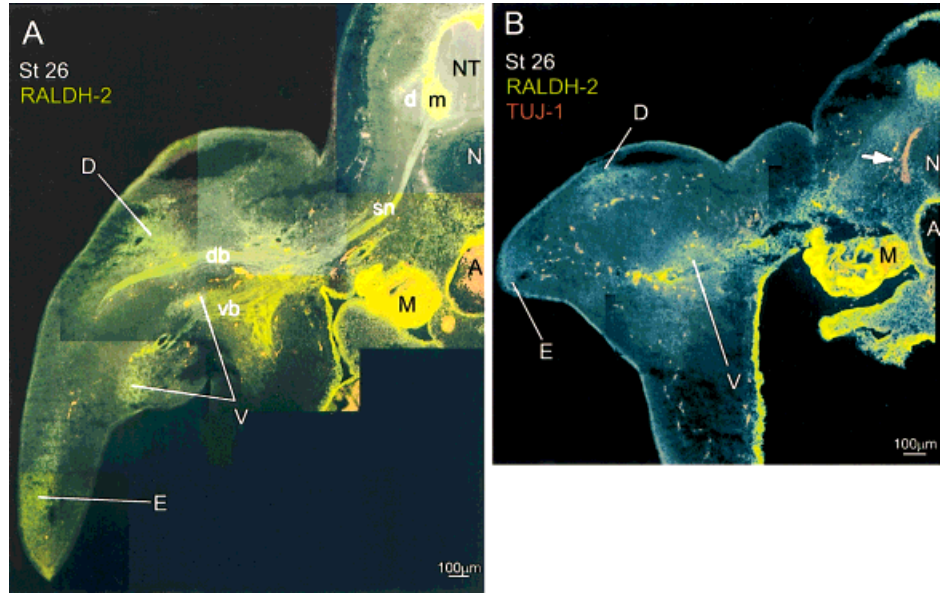


Fig. 7. Retinaldehyde dehydrogenase type 2 immunoreactivity (RALDH-2-IR) in the motor neuron pool of the spinal cord is not altered by changes in peripheral axon targets. **A:** Stage (St) 25 embryo after removal of the limb field on the right side. Yellow line indicates the end of the remaining wing stump. m, motor neuron pools; d, dorsal root ganglion; double arrows, spinal nerve; bp, brachial plexus. **B:** Stage 25 neural tube section after application of a citral bead (b) at stage 15. **C:** Stage 18 neural tube section 24 hr after application of a citral bead (b) at stage 15. The motor neuron pool (arrows) is not altered by the citral application. **D:** Stage 18 neural tube 24 hours after somite deletion and insertion of millipore filter (f). Motor neurons (arrows) are symmetrical on the experimental and control sides. RALDH-2-IR is strong in the meninges and other tissues adjacent to the neural tube.

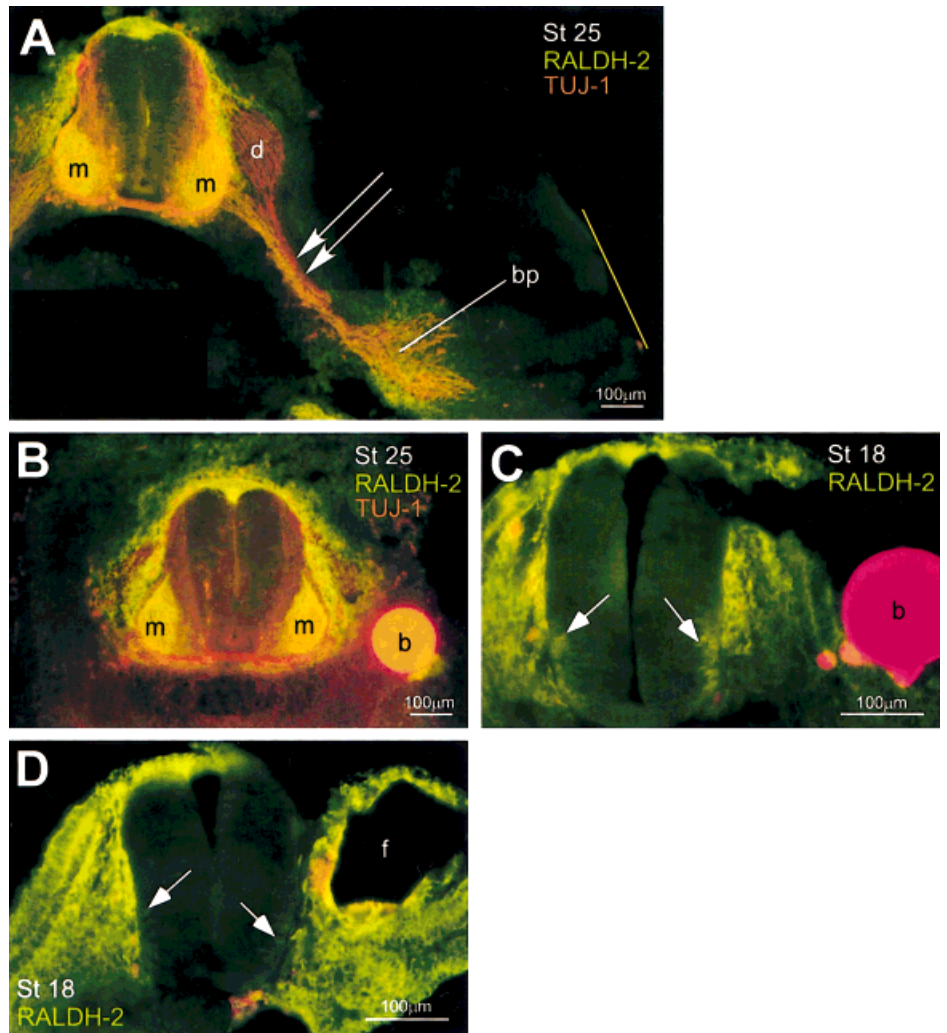


TABLE 2. Decrease in RALDH-2-IR in Wing Mesenchyme Following Wing Denervation^a

Parameter	Limb area (μm^2)	RALDH-2-IR area (μm^2)
Denervated	$(4.38 \pm 0.45) \times 10^7$	$(8.21 \pm 2.17) \times 10^5$
Control	$(4.54 \pm 1.2) \times 10^7$	$(27.1 \pm 6.7) \times 10^5$

^aAreas are given as mean \pm SD, $n = 4$. Limb area indicates total cross-sectional area of the wing. Mann-Whitney rank sum test, $P = 0.0286$ for RALDH-2-IR area. The difference in limb area was not statistically significant. RALDH-2-IR, retinaldehyde dehydrogenase type 2 immunoreactivity.

innervation and can be increased by increasing the levels of vascularization. We were unable to grow limbs in the absence of both neurons and blood vessels. Previous experiments growing limbs in culture have included segments of the spinal cord and central vasculature (Tanaka et al., 1996), thus, these tissues are likely to be necessary for normal wing outgrowth.

Control of RALDH-2-IR in the Motor Neuron Pool

Finally, we investigated control of RALDH-2-IR in the brachial motor neurons, as the axons of these motor neurons contribute a major source of RALDH-2-IR in the wing. A detailed discussion of the patterns of RALDH-2-IR seen in the motor neurons has been presented previously (Socanathan and Jessell, 1998; Berggren et al., 1999). However, it is not clear whether this expression is independent of interactions with target tissues. Similarly, whether RA encountered in the periphery by motor axons induces RALDH-2-IR within the motor neuron pool is unknown. To investigate these possibilities, two approaches were taken. First, the final targets of the motor axons were removed by surgical removal of the limb field at stages 17–18. Embryos were assayed at stage 25, when the motor axons would normally encounter the dorsal and ventral muscle masses of the wing. Although their targets in the wings were absent, RALDH-2-IR in the brachial motor neuron cell bodies remained unchanged compared with unoperated contralateral controls (Fig. 7A). The possibility remains that RA acts to induce or maintain RALDH-2 expression in the motor neurons. Although limbs were absent in these embryos, there was still significant RALDH-2-IR in the brachial plexus, an intermediate target area for the nerve, which could expose motor axons to RA. To determine whether the RA generated in the brachial plexus is influencing the RALDH-2-IR in the motor neuron pool, beads releasing citral, a competitive inhibitor of RALDH-2 and RA synthesis inhibitor, were implanted into the exposed brachial plexus region at several times after the removal of the limb field. Inhibition of RA synthesis in the brachial plexus did not reduce the RALDH-2-IR in the target-deprived motor neuron pool, compared with contralateral controls (not shown).

To determine whether RA encountered in the somites as the motor neurons first exit the neural tube

is inducing the RALDH-2-IR in the motor neuron pool, somites were treated at stage 15 with citral beads to inhibit the synthesis of RA. Although this treatment is known to affect the sympathetic preganglionic neuronal population in the spinal cord (Forehand et al., 1998), we saw no effect on the RALDH-2-IR motor neuron pool at stage 25 (Fig. 7B) or stage 18 (Fig. 7C). In addition to treating the somites with citral, we also performed somite deletions, to determine whether other unspecified somitic factors are influencing RALDH-2 expression in the motor neuron pool. Presomitic tissue was removed before the birth of the motor neurons, but there was no detectable effect on the RALDH-2-IR in the motor neuron pool (Fig. 7D). In this experiment, it should be noted that the tissue that filled in the space of the removed somites was also RALDH-2-IR, so could be providing an alternate source of RA to the neural tube. Additionally, in all of these manipulations, the spinal meninges remain intact, and are a potential source of RA exposure for the spinal cord (see Table 1).

These experiments in aggregate indicate that the expression of RALDH-2 by motor neurons is not influenced by either their final (wing muscle) or intermediate targets (somites). The citral experiments also suggest that externally synthesized RA is not required for continued RALDH-2 expression in motor neurons.

DISCUSSION

We have examined localization of the RA synthetic enzyme RALDH-2 in the developing chicken wing from stages 17 to 30. At stages 17 and 18, RALDH-2-IR is strongly present throughout the wing bud and then is rapidly down-regulated so that, by stage 20, it is not detectable. Retinoic acid is required in the initial specification of axial patterning in the wing; however, we do not find a pattern of RALDH-2-IR within the wing itself that could be providing the required early posterior source. As we have suggested previously, structures near the wing, including the lateral mesoderm and the lateral membrane adjacent to the wing, could be providing the local source of RA involved in this early anterior-posterior patterning (Berggren et al., 1999). By stage 22, RALDH-2-IR is again present in the wing bud, restricted to the presumptive brachial plexus region; this region is strongly immunoreactive for RALDH-2 by stage 23, when axons reach the brachial plexus, and remains so through stage 30. This proximal RALDH-2-IR may provide a continuing source of RA necessary for maintenance of proximal regions of the developing limb (Mercader et al., 2000). Between stages 23 and 30, localized regions of RALDH-2 expression develop in the mesenchyme along the vasculature and nerve branches; this RALDH-2-IR is partially under the control of the blood vessels and motor axons as they enter the wing. This later regional expression of RALDH-2 provides localized sources of RA in the limb during the period of mesenchymal specification. As RA is known to be involved in many aspects of cellular

differentiation, we propose that the RA synthesized locally by RALDH-2 in the wing is involved in the specification of mesenchymal tissues of the limb, including cartilage, skeletal muscle, and vascular smooth muscle.

RALDH-2-IR is present in the area of the developing muscle masses but is not in the myogenic tissues themselves. Our findings that RALDH-2-IR has some overlap with the expression domain of tenascin and that RALDH-2-IR is found in the spaces between desmin- and myosin-immunoreactive cells suggests that RALDH-2 may be localized to connective tissue cell types. However, it is also possible that RALDH-2 expression is restricted to undifferentiated cell types and is lost as the tissues differentiate into immunohistochemically identifiable cell types.

RALDH-2-IR in motor axons is observed throughout axon outgrowth into the premuscle masses. RA can be released from these motor neurons, and the implications of this source of RA in the wing are discussed below. The loss of RALDH-2-IR in the wing mesenchyme after denervation strongly implicates the motor axons as a source of RA and/or a source of RALDH-2 induction in the wing. Another source of RALDH-2 in the wing is the blood vessels, which also release RA and which can act as another source of endogenous RA and/or RALDH-2 induction. The identification of these sites of RA synthesis in the wing broadens our understanding of the control of endogenous RA in limb development.

Locally Synthesized RA and Cartilage Development

Before this report, a source for RA in the limb has not been identified at the time that cartilage is forming, although studies of cartilage development indicate a role for RA in the formation of cartilaginous structures. Chondrocytes express RA receptors in conjunction with high levels of retinoids in cartilage and perichondrial tissues (Koyama et al., 1999). In addition, chondrogenic cells in culture are unable to fully mature in the absence of RA (Oettinger and Pacifici, 1990; Iwamoto et al., 1993a,b). The administration of excess RA decreases chondrocyte proliferation and hypertrophy; these effects are blocked by RAR antagonists (De Luca et al., 2000). Overexpression of a constitutively active RAR α (Weston et al., 2000) indicates that RA is necessary for initial induction of prechondrogenic tissues but then must be excluded for the tissues to continue differentiation. These animals showed many of the same skeletal deformities as the RAR α and RAR γ null alleles (Lohnes et al., 1994). RA negatively regulates growth plate chondrogenesis, thus inhibiting long bone outgrowth (De Luca et al., 2000). Inhibition of RA receptors in the region of the long bones of the wing also alters outgrowth of cartilaginous structures (Koyama et al., 1999). In addition, RA is necessary for posthypertrophic mineralization of cartilage, an essential step in the transition from cartilage to mature bone

(Koyama et al., 1999). Evidence from these and other studies strongly suggest a role for RA in coordinating the timing of chondroblast formation as well as cartilage morphogenesis.

A role for locally synthesized RA in the maturation of cartilage is suggested by the use of the RA synthesis inhibitor citral, which blocks both steps of synthesis of RA from retinol (vitamin A) (Connor and Smit, 1987; Kikonyogo et al., 1999). Treatment of limbs with citral (Tanaka et al., 1996) shows wing defects similar to those in studies using RA receptor knockouts (Lohnes et al., 1994). Administration of a retinoic acid antagonist to the wing bud results in shortened and/or malformed long bones within the mature wing (Mercader et al., 2000). The above studies indicate that locally synthesized RA plays a role in the specification, morphology, and outgrowth of limb cartilage. Here, we report RALDH-2-IR in the developing limb at the time of initial cartilage condensation. Thus, RA synthesis could be playing an important role in localization of initial cartilage condensation, as well as guiding the later outgrowth of the cartilage as it mineralizes and matures.

Because the motor neurons are a potential source of RALDH-2 in the limb, it is possible that the nerve is indirectly affecting cartilage growth. The similarity between the defects seen with limb denervation and with RA receptor knockouts supports a link between the nerve, locally synthesized RA in the limb, and cartilage growth.

Locally Synthesized RA and Muscle Specification

Retinoic acid induces a neuronal phenotype in P19 embryonal carcinoma cells (Jones-Villeneuve et al., 1982), but experiments with a subclone of these cells demonstrate that RA can induce several different cell fates, depending on the concentration (Edwards and McBurney, 1983). At lowest concentrations, cardiac muscle cells were induced, and at higher concentrations (although lower than required to induce neuronal phenotype), skeletal myoblasts and myotubes are observed. This differentiation of skeletal muscle and the accompanying decrease in proliferation has been found to be dependent on the RAR α receptor in adult skeletal muscle and myogenic cells (Halevy and Lerman, 1993). RA can also inhibit myogenesis in mammalian culture systems (Xiao et al., 1995). That exposure of myogenic cells to RA at different developmental times results in variable outcomes is not surprising, because RA is a morphogen requiring precise spatiotemporal regulation.

During wing formation, the dorsal and ventral pre-muscle masses are established in the wing between stages 20 and 23 (Schramm and Solursh, 1990), a time when RALDH-2-IR is not detectable in the limb mesenchyme. Myogenic cells differentiate into immunohistologically recognizable muscle at stage 25, the stage when they encounter motor neurons migrating into the

limb (Landmesser, 1978, Sweeney et al., 1989). At stage 25 we show RALDH-2-IR in the limb mesenchymal tissue surrounding the RALDH-2-IR nerves and blood vessels entering the wing. As we have shown that these tissues are capable of releasing RA, there are two potential sources of RA in the wing muscle masses: RA from RALDH-2-containing mesenchymal cells, and RA released from RALDH-2-containing motor axons. These sources of RA could influence the differentiation of skeletal muscle cells, the proliferation of muscle fibers, and the recruitment of mesenchymal cells into the skeletal muscle groups.

Locally Synthesized RA and Vascular Smooth Muscle Development

Retinoic acid released by blood vessel walls may play a role in the maturation of the blood vessels themselves through a recruitment of surrounding cells to a smooth muscle phenotype. Several studies have demonstrated that RA is involved in the regulation of smooth muscle cell differentiation and proliferation. RA induces smooth muscle morphology, gene expression, and contractility in P19 embryonal carcinoma cells (Blank et al., 1995; Suzuki et al., 1996). Additionally, an RA-response element linked to *lacZ* expression has demonstrated colocalization of RA and smooth muscle cells in the developing ductus arteriosus (Colbert et al., 1996), whereas RA receptors are involved in the regulation of smooth muscle cell growth (Miano et al., 1996). Our localization of the RALDH-2 enzyme in the smooth muscle cells of the vasculature is consistent with a role for endogenous RA in blood vessel formation.

Regulation of RALDH-2

The role of RA in regulation of RALDH-2 is still unclear. If RA is inducing differentiation of cell types in the wing tissues examined here, it follows that RALDH-2 may be one of the genes expressed by the induced cells following their specification by RA. Therefore, RA could induce up-regulation of RALDH-2 through an inductive differentiation pathway. Additional regulation of RALDH-2 in the wing could be through interaction with an FGF pathway. RA induces the proximalizing gene *Meis*, which appears to be restricted to the proximal wing bud by the activity of FGF8 released from the AER (Mercader et al., 2000). FGF8 may be controlling RA in the wing through regulation of RALDH-2 expression and may be responsible for the loss of RALDH-2-IR seen between stages 17 and 20. Furthermore, although proximal RA synthesis may continue due to RALDH-2 expression in the brachial plexus region, generalized RALDH-2 expression is inhibited by FGF signaling more distally (Mercader et al., 2000). Thus, the vascular and neuronal regulation of RALDH-2 within specific regions of the limb mesenchyme may be crucial for providing localized RA for differentiation of structures within the limb.

CONCLUSIONS

We have presented evidence that the expression of the RA synthetic enzyme RALDH-2 in the mesenchyme is at least partially under the control of the motor axons and vasculature during the development of the avian wing. We also demonstrate that these tissues are capable of releasing RA into the limb mesenchyme, thus, providing a major source of RA to these tissues. RALDH-2 has been shown to be up-regulated by its endproduct, RA (Zhao et al., 1996); thus, it is possible that the RA entering the wing with innervation and vasculature is inducing additional RALDH-2 expression in the mesenchyme. This induction could be direct, as RALDH-2 is known to have a RA response element in its *cis*-regulatory region (Zhao et al., 1996), or up-regulation of RALDH-2 could be through a differentiation pathway, whereby RA induces differentiation to cell types that then express RALDH-2. As RA is a potent mediator of cellular differentiation, RA released by RALDH-2 expressing tissues may specify differentiation of limb mesenchymal tissues during development. It is important to note that activity of RALDH-2 must be compared with RA degradation in making a final determination of roles for RA in any developmental system. Enzymes involved in degrading RA have been studied recently (Yamamoto et al., 1998; de Roos et al., 1999; McCaffery et al., 1999; Swindell et al., 1999), although not in the stages of the wing examined here. As suggested by Swindell et al. (1999), RA synthesis by RALDH-2 could be acting in balance with RA degradation to create a "developmental switch" that regulates genes responsible for various aspects of limb morphogenesis. If some of this RA-mediated differentiation is under the control of innervation and vasculature, there are broad implications for the role of motor nerves and blood vessels in the development of many other systems of the body.

EXPERIMENTAL PROCEDURES

Immunohistochemistry

Fertilized White Leghorn chicken eggs were supplied from Oliver Merrill and Sons of Londonderry, New Hampshire. Eggs were stored at 4°C then incubated at 37°C for 3–6 days. Embryos were staged according to the normal series of Hamburger and Hamilton (H&H) (Hamburger and Hamilton, 1951). Stage 17–29 chicken embryos were collected and fixed in 4% paraformaldehyde overnight, cryoprotected in 30% sucrose, embedded in OCT (Tissue-Tek) for freezing at –30°C and sectioned at 30 μm on the cryostat. Sections were incubated overnight in 1:2,500 rabbit anti-RALDH-2 preabsorbed with chicken liver acetone powder (Sigma) (as described in Berggren et al., 1999). Goat anti-rabbit fluorescein isothiocyanate-labeled secondary antibody (ICN/Cappel) was used at a 1:500 dilution for visualization of RALDH-2. All secondary antibodies were diluted in 0.3% Triton X-100 (Sigma) in phosphate buffered saline (PBS).

TABLE 3. Summary of Primary Antibodies Used

Primary antibody and dilution ^a	Protein or cell type visualized by this antibody	Source of antibody
1:250 TUJ-1	Neural specific tubulin	Berkeley Antibody Co.
1:10 ALD66	Slow muscle yosin	Donald Fischman, DSHB ^b
1:50 Pax-7	Migrating premyogenic cells	Atsushi Kawakami, DSHB ^b
1:10 Desmin	Intermediate filaments in unspecified muscle	Donald Fischman, DSHB ^b
1:1 Tenascin	Early connective tissue	Douglas Fambrough, DSHB ^b
1:100 α -smooth muscle actin	Smooth muscle cells	Sigma

^aPrimary antibodies were diluted in 0.3% Triton in PBS. Tissues were incubated overnight at 4°C. For all antigens other than RALDH-2, either rhodamine-labeled goat anti-mouse secondary antibody (Kirkegaard & Perry Labs) was used at 1:50, or Cy3-labeled goat anti-mouse secondary antibody (Jackson labs) was used at 1:200.

^bDevelopmental Hybridoma Bank, maintained by the University of Iowa, Department of Biological Sciences, Iowa City, IA 52242, under contract No1-HD-7-3263 from the NICHD. Developer of the antibody is listed first.

Other antibodies used are summarized in Table 3. Tissue sections were either viewed with a Nikon fluorescence microscope and photographed on slide film or viewed with a Bio-Rad MRC 1024ES confocal scanning laser microscope mounted on an Olympus BX50 upright light microscope, and images were collected by using LaserSharp software. The confocal microscopy was performed in the Cell Imaging Facility at the University of Vermont College of Medicine. All images were digitized and imported into Adobe Photoshop for image optimization and montage construction.

Isolation and Culture of Motor Neurons

Motor neurons were purified from chicken embryos as follows: whole spinal cords were dissected from embryos incubated for 6 days (E6), rinsed in dissection buffer consisting of Hanks' balanced salt solution (Gibco) with 1 mM sodium pyruvate and 10 mM HEPES buffer (Gibco), and held in Neurobasal media (Gibco) with B27 supplement (Gibco). Typically, 8–20 spinal cords were dissected per experiment, then grouped, combined, and incubated in dissociation media (0.05% trypsin in EDTA with 0.02% DNase I) for 15 min at 37°C. Dissociation was interrupted by the addition of 10% fetal calf serum (Gibco) in Neurobasal media, and spinal cords were mechanically separated by trituration through the a narrow-bore, fire-polished Pasteur pipette. Isolation of motor neurons was based on the protocol of Becker et al. (1998). Briefly, the single-cell suspension was layered onto 5 ml of Neurobasal media and centrifuged at $100 \times g$ for 5 min to remove debris. Pelleted cells were resuspended in 1 ml of Neurobasal media and layered onto 4 ml of 26.7% (w/v) Nycodenz (Gibco) in HBSS and centrifuged at $400 \times g$ for 10 min. The intermediate layer was collected and resuspended at a density of 10^6 cells/ml in serum-free plating media, consisting of Neurobasal media with B27 supplement (Gibco), 0.5 mM L-glutamine (Sigma), 25 μ M glutamate (Sigma), and 10 ng/ml Carditrophin-1 (Leinco Technologies, Inc., St. Louis, MO). Motor neurons from the hindbrains of the same animals were isolated according to the same protocol and used as a control, as the hindbrain sections show no detectable RALDH-2-IR at this stage.

Smooth Muscle Cell Cultures

Cultured vascular smooth muscle cells were a gift of Dr. Deborah Damon of the Department of Pharmacology, University of Vermont. Cells were isolated from explants of adult Sprague Dawley rat aortas according to the protocol of Ross (1971). Cells exhibited characteristic "hill and valley" growth patterns and immunohistochemical labeling with a monoclonal antibody for smooth muscle-specific α -actin. Vascular cells were grown in low glucose DMEM supplemented with 10% fetal bovine serum (FBS), 1 mM glutamine, 100 IU of penicillin, and 100 IU of streptomycin. Cells were fixed with 4% paraformaldehyde overnight, and stored in PBS until stained according to procedures given above.

Determination of RA Synthetic Ability of RALDH-2-IR Tissues

Motor axons and blood vessels are two strongly RALDH-2-IR tissues that extend into the wing between stages 23 and 25 of chicken development. To determine whether these tissues have the capacity to release RA into the wing tissue, RA reporter cells (Sil-15 RA reporter cell line from Dr. M. Wagner) were used in a culture system assay previously described by McCaffery and Dräger (1997). Because not all cells will maintain expression of the lacZ gene after subsequent passages, there is a weakening of response with older cells. Therefore, our assays always compared experimental and control tissues by using responsive cells of the same passage. Tissues of interest, either isolated motor neurons or dissected blood vessels from the CAM, were incubated overnight in 200 μ l of L15 media (Sigma), then centrifuged and the supernatant withdrawn. The supernatants were then added to the cultured reporter cells, which are F9 teratocarcinoma cells transfected with the RA response element (RARE) from the RAR β driving expression of a β -galactosidase reporter (Wagner et al., 1992). The cells were incubated overnight, fixed, and reacted for β -gal reaction product, which was analyzed colorimetrically for a semiquantitative measure of RA synthesis (McCaffery and Dräger, 1997). The amount of RA synthesized was determined by reference to a standard curve. It is important to note that

this procedure is based on comparison of response to tissues processed together, rather than on a quantitative absolute value, so results from a single run cannot be compared with subsequent trials.

Motor neurons and blood vessels were also cocultured with Sil-15 reporter cells in tissue culture dishes to illustrate RA release from motor neuron cell bodies and axons. Motor neurons were plated in serum-free media at a density of 1×10^6 cells/ml into 35-mm tissue culture dishes according to the procedure outlined above. To find a substrate suitable for both the motor neurons and the Sil-15 cells, several different ones were compared. Dishes were treated with either gelatin (0.2%, incubated at room temperature for 1 hr), collagen (rat tail collagen courtesy of Dr. Carson Cornbrooks diluted 1:3 in sterile water and dried on dishes in a laminar flow hood), or laminin (Sigma, 2 μ g/ml, incubated for 1 hr at room temperature). Laminin coating allowed for the best growth of both the motor neurons and the reporter cells, although collagen-coated plates were used for some of the experimental dishes as well. All dishes were rinsed with sterile PBS before plating cells. The cocultures were performed according to one of two protocols: (1) motor neurons were either plated onto preexisting lawns of Sil-15 cells (grown to confluence) and incubated overnight, after which the cells were fixed, reacted for β -gal reaction product, and photographed as whole dishes with a Nikon Coolpix 990 digital camera; or, (2) motor neurons were grown for 2 days alone to allow for the extension of processes, after which Sil-15 cells were added at a lower density (2.4×10^5 cells/dish), and allowed to grow overnight before being fixed and reacted. Samples of each dish were photographed through a Nikon Diaphot inverted phase-contrast microscope, to observe where the responsive cells were localized in relation to the cultured neurons. CAM blood vessel sections were placed on confluent layers of responsive cells and incubated overnight, after which the tissue samples were removed and the cells were fixed and reacted as above.

Growth of Wings on the Chorioallantoic Membrane

To examine the distribution of RALDH-2-IR in the absence of innervation, limb buds were removed from the embryo before innervation and grown on the CAM of host embryos. Wing buds were dissected from stage 18–19 embryos into physiological saline and kept on ice until ready to transplant. The wings were dissected with sharpened tungsten needles to avoid compressing the tissue at the root of the limb. Wings were then grafted onto the CAM of embryonic day (E) 10 embryos as follows. The host embryos were windowed at E3, then just before grafting, small capillaries of the CAM were gently torn with sharpened tungsten needles at the site of the graft. The grafted wings were aligned over the area of bleeding, and excess saline removed with a Pasteur pipette. The eggs were then returned to the incubator for 3–5 days, and the grafts were re-

moved and fixed when their morphology resembled that of either stage 25 or 28 control wings. Limb buds were staged based on their morphology, rather than the time since grafting, because it takes some time for the graft to adhere to the CAM and reinitiate growth. After fixation, the wings were sectioned and stained for RALDH-2-IR as described above for whole embryos.

Denervation of Embryonic Wings and Analysis of RALDH-2-IR Area

To determine whether the RALDH-2-IR in the wing is dependent on innervation by motor axons, embryos were denervated in the brachial region. Denervation was accomplished by removing the neural tubes of embryos at H&H stage 15–16, a time in development when the neural crest has already migrated, but the motor neurons have not yet begun to grow out of the neural tube (Landmesser, 1978). The neural tubes were removed by gentle suction after making cuts between the neural tube and somite with sharpened tungsten needles. After neural tube removal, the eggs were returned to the incubator for 2–4 days and killed and fixed at H&H stage 25 or 28. Embryos were then sectioned and stained for RALDH-2-IR as described above.

Analysis of the area of RALDH-2-IR in the denervated wings was performed by using the Lucivid camera system and NeuroLucida software (MicroBrightField, Inc.). The area of mesenchymal RALDH-2-IR was traced in each section through the wing in denervated and control embryos, and the total area of RALDH-2-IR calculated with NeuroExplorer numerical analysis. This area was compared with the total wing volume for both the denervated and control embryos. To determine significance of the differences in RALDH-2-IR area, a Mann-Whitney rank sum test was used (SigmaStat software, Jandel Scientific).

Exogenous Application of Citral and Axon Target Removals

Citral is a competitive inhibitor of RA synthesis by aldehyde dehydrogenase-mediated oxidation (Chen et al., 1995; Connor and Smit, 1987), and was used to determine whether RA synthesis in the somites is necessary for specification of RALDH-2-IR motor neurons in the neural tube. Citral was applied to the somites following the protocol of Forehand et al. (1998). Briefly, H&H stage 12 embryos were exposed by cutting a small window in the shell and citral applied to individual somites by using a slow-release bead delivery system (Tickle et al., 1985). Three anion exchange resin beads soaked in 10^{-4} M citral in dimethyl sulfoxide (DMSO) were placed on the last somite and the presomitic tissue equivalent to the next two somites (approximately somites 16, 17, and 18 of a 16 somite embryo). These are segments that contribute to the formation of the brachial plexus, innervate the wing, and show RALDH-2-IR in their motor neuron pool (Berggren et al., 1999). Control beads for these experiments were soaked in the

vehicle, DMSO. Beads (AG1-X2, 200–400 mesh, Bio-Rad) were 50–100 μm in diameter and, thus, smaller than an individual somite. Eggs were then closed by sealing a glass coverslip over the window with paraffin, and embryos were reincubated and allowed to mature to stage 18 or 25 at which time they were fixed, sectioned, and stained for RALDH-2-IR as above, and the size of the RALDH-2-IR motor neuron pool was analyzed.

Somites adjacent to the brachial neural tube were removed to assess whether the newly formed somites were releasing factors other than RA that were influencing RALDH-2 expression of the motor neuron pool. Presomitic tissue approximately 4 somites ahead of the last formed somite was removed in 14 or 15 somite embryos. Presomitic tissue was determined by removing a section of mesoderm at least as wide as the already formed somites, and the full depth of the somatopleure. This is tissue that shows strong RALDH-2-IR throughout somitic development (Berggren et al., 1999). Tissue was removed by cutting with tungsten needles and gentle suction. The space left was filled with a small piece of millipore filter to prevent the somitic tissue filling in, although some filling in by adjacent tissues did occur. These embryos were allowed to mature to stage 18, at which time they were sectioned and stained for analysis as above.

To further examine the role of target tissue on the RALDH-2 expression of the motor neurons, the entire limb field was removed as soon as it became distinct, at stage 17. Tungsten needles were used to make transverse cuts lateral to somites 15 and 20, then used to dissect away the lateral plate mesoderm between them. Tissue was taken from just lateral to the somites and removed as far ventrally as possible. In a subset of these animals, the limb removals were followed by the application of citral beads (as described above). The beads were implanted by making small cuts with a tungsten needle, after which three or four beads were placed into the approximate center of the limb stump, close to the presumptive brachial plexus.

ACKNOWLEDGMENTS

The authors thank Dr. Deborah Damon for the gift of cultured smooth muscle cells, as well as advice about vascular development. We also thank Dr. Carson Cornbrooks for the gift of rat tail collagen, help with cell culture protocols, and helpful comments on the manuscript. In addition, we thank Casey Johnson, Darien Crimmen, and Derek Moody for technical assistance. C.J.F. and P.M. received support from the NIH.

REFERENCES

- Becker E, Soler RM, Yuste VJ, Giné E, Sanz-Rodríguez C, Egea J, Martín-Zanca D, Comella JX. 1998. Development of survival responsiveness to brain-derived neurotrophic factor, neurotrophin 3 and neurotrophin 4/5, but not to nerve growth factor, in cultured motoneurons from chick embryo spinal cord. *J Neurosci* 18:7903–7911.
- Berggren K, McCaffery P, Dräger U, Forehand CJ. 1999. Differential distribution of retinoic acid synthesis in the chicken embryo as determined by immunolocalization of the retinoic acid synthetic enzyme, RALDH-2. *Dev Biol* 210:288–304.
- Blank RS, Swartz EA, Thompson MM, Olson EN, Owens GK. 1995. A retinoic acid-induced clonal cell line derived from multipotential P19 embryonal carcinoma cells expresses smooth muscle characteristics. *Circ Res* 76:742–749.
- Chen H, Namkung MJ, Juchau MR. 1995. Biotransformation of all-trans-retinol and all-trans-retinal to all-trans-retinoic acid in rat conceptual homogenates. *Biochem Pharmacol* 50:1257–1264.
- Colbert M, Kirby M, Robbins J. 1996. Endogenous retinoic acid signaling colocalizes with advanced expression of the adult smooth muscle myosin heavy chain isoform during development of the ductus arteriosus. *Circ Res* 78:790–798.
- Connor M, Smit M. 1987. Terminal-group oxidation of retinol by mouse epidermis. Inhibition in vitro and in vivo. *Biochem J* 244:489–492.
- De Luca F, Uyeda J, Mericq V, Mancilla E, Yanovski J, Barnes K, Zile M, Baron J. 2000. Retinoic acid is a potent regulator of growth plate chondrogenesis. *Endocrinology* 141:346–353.
- de Roos K, Sonneveld E, Compaan B, ten Berge D, Durston A, van der Saag P. 1999. Expression of retinoic acid 4-hydroxylase (CYP26) during mouse and *Xenopus laevis* embryogenesis. *Mech Dev* 82:205–211.
- Dietz F. 1987. Effect of peripheral nerve on limb development. *J Orthop Res* 5:576–585.
- Dollé P, Izpisua-Belmonte J-C, Falkenstein H, Renucci A, Duboule D. 1989. Coordinate expression of the murine *Hox-5* complex homeobox-containing genes during limb pattern formation. *Nature* 342:767–772.
- Dollé P, Fraulob V, Kastner P, Chambon P. 1994. Developmental expression of murine retinoid X receptor (RXR) genes. *Mech Dev* 45:91–104.
- Edwards M, McBurney M. 1983. The concentration of retinoic acid determines the differentiated cell types formed by a teratocarcinoma cell line. *Dev Biol* 98:187–191.
- Eichele G. 1989. Retinoic acid induces a pattern of digits in anterior half wing buds that lack the zone of polarizing activity. *Development* 107:863–867.
- Forehand CJ, Ezerman EB, Goldblatt JP, Skidmore DL, Glover JC. 1998. Segment-specific pattern of sympathetic preganglionic projections in the chicken embryo spinal cord is altered by retinoids. *Proc Natl Acad Sci USA* 95:10878–10883.
- Fredette BJ, Landmesser LT. 1991. A reevaluation of the role of innervation in primary and secondary myogenesis in developing chick muscle. *Dev Biol* 143:19–35.
- Goulding M, Gruss P. 1989. The homeobox in vertebrate development. *Curr Opin Cell Biol* 1:1088–1093.
- Halevy O, Lerman O. 1993. Retinoic acid induces adult muscle cell differentiation mediated by the retinoic acid receptor- α . *J Cell Physiol* 154:566–572.
- Hamburger V, Hamilton HL. 1951. A series of normal stages in the development of the chick embryo. *J Morphol* 88:49–92.
- Helms JA, Kim CH, Eichele B, Thaller C. 1996. Retinoic acid signaling is required during early chick limb development. *Development* 122:1385–1394.
- Hirschi KK, Rohovsky SA, D'Amore PA. 1998. PDGF, TGF-, and heterotypic cell-cell interactions mediate endothelial cell-induced recruitment of 10T1/2 cells and their differentiation to a smooth muscle fate. *J Cell Biol* 141:805–814.
- Iwamoto M, Golden E, Adams S, Noji S, Pacifici M. 1993a. Responsiveness to retinoic acid changes during chondrocyte maturation. *Exp Cell Res* 205:213–224.
- Iwamoto M, Shapiro I, Yagami K, Boskey A, Leboy P, Adams S, Pacifici M. 1993b. Retinoic acid induces rapid mineralization and expression of mineralization-related genes in chondrocytes. *Exp Cell Res* 207:413–420.
- Jones-Villeneuve E, McBurney M, Rogers K, Kalnins V. 1982. Retinoic acid induces embryonal carcinoma cells to differentiate into neurons and glial cells. *J Cell Biol* 94:253–262.

- Karden G. 1998. Muscle and tendon morphogenesis in the avian hind limb. *Development* 125:4019–4032.
- Kikonyogo A, Abriola DP, Dryjanski M, Pietruszko R. 1999. Mechanism of inhibition of aldehyde dehydrogenase by citral, a retinoid antagonist. *Eur J Biochem* 262:704–712.
- Koyama E, Golden EB, Kirsch T, Adams SL, Chandraratna RAS, Michaille J-J, Pacifici M. 1999. Retinoid signaling is required for chondrocyte maturation and endochondral bone formation during limb skeletogenesis. *Dev Biol* 208:375–391.
- Landmesser L. 1978. The distribution of motoneurons supplying chick hind limb muscles. *J Physiol (Lond)* 284:371–389.
- Lohnes D, Kastner P, Dierich A, Mark M, LeMeur M, Chambon P. 1993. Function of retinoic acid receptor γ in the mouse. *Cell* 73:643–658.
- Lohnes D, Mark M, Mendelsohn C, Dollé P, Dierich A, Gorry P, Gansmuller A, Chambon P. 1994. Function of the retinoic acid receptors (RARs) during development: I. Craniofacial and skeletal abnormalities in RAR double mutants. *Development* 120:2723–2748.
- Lu H-C, Eichele G, Thaller C. 1997. Ligand-bound RXR can mediate retinoid signal transduction during embryogenesis. *Development* 124:195–203.
- Maden M, Sonneveld E, van der Saag PT, Gale E. 1998. The distribution of endogenous retinoic acid in the chick embryo: implications for developmental mechanisms. *Development* 125:4133–4144.
- McCaffery P, Dräger UC. 1994. Hot spots of retinoic acid synthesis in the developing spinal cord. *Proc Natl Acad Sci USA* 91:7194–7197.
- McCaffery P, Dräger U. 1997. A sensitive bioassay for enzymes that synthesize retinoic acid. *Brain Res Protocols* 1:232–236.
- McCaffery P, Wagner E, O'Neil J, Petkovich M, Dräger UC. 1999. Dorsal and ventral retinal territories defined by retinoic acid synthesis, break-down and nuclear receptor expression. *Mech Dev* 85:203–214.
- Mendelsohn C, Ruberte E, LeMeur M, Morriss-Kay G, Chambon P. 1991. Developmental analysis of the retinoic acid-inducible RAR-beta 2 promoter in transgenic animals. *Development* 113:723–734.
- Mendelsohn C, Lohnes D, Décimo D, Lufkin T, LeMeur M, Chambon P, Mark M. 1994. Function of the retinoic acid receptors (RARs) during development: II. Multiple abnormalities at various stages of organogenesis in RAR double mutants. *Development* 120:2749–2771.
- Mercader N, Leonardo E, Piedra ME, Martinez-A C, Ros MA, Torres M. 2000. Opposing RA and FGF signals control proximodistal vertebrate limb development through regulation of Meis genes. *Development* 127:3961–3970.
- Miano J, Topouzis S, Majesky M, Olson E. 1996. Retinoid receptor expression and all-trans retinoic acid-mediated growth inhibition in vascular smooth muscle cells. *Circulation* 93:1886–1895.
- Niederreither K, McCaffery P, Dräger UC, Chambon P, Dollé P. 1997. Restricted expression and retinoic acid-induced downregulation of the retinaldehyde dehydrogenase type 2 (RALDH-2) gene during mouse development. *Mech Dev* 62:67–78.
- Niederreither K, Subbarayan V, Dollé P, Chambon P. 1999. Embryonic retinoic acid synthesis is essential for early mouse post-implantation development. *Nat Genet* 21:444–448.
- Oettinger H, Pacifici M. 1990. Type X collagen gene expression is transiently up-regulated by retinoic acid treatment in chick chondrocyte cultures. *Exp Cell Res* 191:292–298.
- Phillips W, Bennett M. 1984. Differentiation of fiber types in wing muscles during embryonic development: effect of neural tube removal. *Dev Biol* 106:457–468.
- Power SC, Lancman J, Smith SM. 1999. Retinoic acid is essential for Shh/Hoxd signaling during rat limb outgrowth but not for limb initiation. *Dev Dyn* 216:469–480.
- Ross R. 1971. The smooth muscle cell: II. Growth of smooth muscle in culture and formation of elastic fibers. *J Cell Biol* 50:172–186.
- Ruberte E, Dollé P, Krust A, Zelent A, Morriss-Kay G, Chambon P. 1990. Specific spatial and temporal distribution of retinoic acid receptor gamma transcripts during mouse embryogenesis. *Development* 108:213–222.
- Schramm C, Solursh M. 1990. The formation of premuscle masses during chick wing bud development. *Anat Embryol (Berl)* 182:235–247.
- Sockanathan S, Jessell TM. 1998. Motor neuron-derived retinoid signaling specifies the subtype identity of spinal motor neurons. *Cell* 94:503–514.
- Stratford T, Horton C, Maden M. 1996. Retinoic acid is required for the initiation of outgrowth in the chick limb bud. *Curr Biol* 6:1124–1133.
- Stratford T, Logan C, Zile M, Maden M. 1999. Abnormal anteroposterior and dorsoventral patterning of the limb bud in the absence of retinoids. *Mech Dev* 81:115–125.
- Suzuki T, Kim H, Kurabayashi M, Hamada H, Fujii H, Aikawa M, Watanabe M, Watanabe N, Sakomura Y, Yazaki Y, Nagai R. 1996. Preferential differentiation of P19 mouse embryonal carcinoma cells into smooth muscle cells. Use of retinoic acid and antisense against the central nervous system-specific POU transcription factor Brn-2. *Circ Res* 78:395–404.
- Sweeney L, Kennedy J, Zak R, Kokjohn K, Kelley S. 1989. Evidence for expression of a common myosin heavy chain phenotype in future fast and slow skeletal muscle during initial stages of avian embryogenesis. *Dev Biol* 133:361–374.
- Swindell EC, Thaller C, Sockanathan S, Petkovich M, Jessell TM, Eichele G. 1999. Complementary domains of retinoic acid production and degradation in the early chick embryo. *Dev Biol* 216:282–296.
- Tanaka M, Tamura K, Ide H. 1996. Citral, an inhibitor of retinoic acid synthesis, modifies chick limb development. *Dev Biol* 175:239–247.
- Thaller C, Eichele G. 1987. Identification and spatial distribution of retinoids in the developing chick limb bud. *Nature* 327:625–628.
- Thaller C, Eichele G. 1990. Isolation of 3,4-didehydroretinoic acid, a novel morphogenetic signal in the chick wing bud. *Nature* 345:815–819.
- Tickle C, Alberts B, Wolpert L, Lee J. 1982. Local application of retinoic acid to the limb bud mimics the action of the polarizing region. *Nature* 296:564–566.
- Tickle C, Lee J, Eichele G. 1985. A quantitative analysis of the effect of all-trans-retinoic acid on the pattern of chick wing development. *Dev Biol* 109:82–95.
- Wagner M, Han B, Jessell TM. 1992. Regional differences in retinoid release from embryonic neural tissue detected by an in vitro reporter assay. *Development* 116:55–66.
- Weston AD, Rosen V, Chandraratna RAS, Underhill TM. 2000. Regulation of skeletal progenitor differentiation by the BMP and retinoid signaling pathways. *J Cell Biol* 148:679–690.
- Xiao Y, Grieshammer U, Rosenthal N. 1995. Regulation of a muscle-specific transgene by retinoic acid. *J Cell Biol* 129:1345–1354.
- Yamamoto M, Dräger UC, McCaffery P. 1998. A novel assay for retinoic acid catabolic enzymes shows high expression in the developing hindbrain. *Dev Brain Res* 107:103–111.
- Zhao D, McCaffery P, Ivins K, Neve R, Hogan P, Chin W, Dräger U. 1996. Molecular identification of a major retinoic-acid-synthesizing enzyme, a retinaldehyde-specific dehydrogenase. *Eur J Biochem* 240:15–22.